The feasibility of in-situ steam injection technology for oil shale underground retorting

Zhiqin Kang[(a,b)*], Huanyu Xie[(a,b)], Yangsheng Zhao[(a,c)], Jing Zhao

(a) State Center for Research and Development of Oil Shale Exploitation, Beijing 100083, China
(b) Key Laboratory of In-situ Property-improving Mining of Ministry of Education, Taiyuan University of Technology, Taiyuan 030024, China
(c) Mining Technology Institute, Taiyuan University of Technology, Taiyuan 030024, China

Abstract: *The basic principles of in-situ steam injection technology (MTI) for oil shale underground retorting were presented and related technical processes were analyzed. The convection heat transfer of steam enhanced the efficiency of heating the oil shale layer, which shortened the time to achieve a complete pyrolysis of organic matter. Under the influence of steam the migration capacity of oil and gas improved and the oil and gas products were carried out of the production well more quickly. Moreover, by using superheated steam (up to 570 °C) to pyrolyze oil shale, the oil recovery rate exceeded 95%, and the gas production per unit mass was 0.041 m³/kg, at the same time, the quality of oil and gas products greatly improved. The proportion of light oils accounted for 75.38%, and the yield of H_2 and CO in pyrolysis gases was increased. The numerical simulation of steam injection indicated that the MTI technology was a rapid and efficient method for oil shale underground retorting to extract oil and gas by using the injection and production wells alternately for injecting steam. It demonstrated that the development period of the MTI technology was only about 300 days for an oil shale reservoir with a well spacing of 50 m, and the roof and floor of the oil shale layer served as thermal and steam insulation. The successful industrial implementation of the MTI technology in the future should alleviate the increasing energy crisis in China and reduce the country's dependence on imported petroleum.*

Keywords: *oil shale underground retorting, in-situ steam injection, superheated steam, energy crisis.*

1. Introduction

Oil shale is an unconventional oil resource that is very abundant globally and is estimated to contain more than 600 billion tons of shale oil, which is more than the world recoverable reserves of crude oil (170 billion tons) [1]. Kerogen

* Corresponding author: e-mail *kangzhiqin810101@126.com*

in oil shale is highly sensitive to variations in temperature during its vigorous thermal decomposition and shale oil and gas production with the temperature increasing from 300 to 550 °C [2–4]. China's shale oil resources are known to be around 47.6 billion tons, being the second largest in the world [5, 6]. At the same time, conventional oil resources cannot meet the rapidly growing oil demand in the country, and therefore, shale oil is likely to play a decisive role in future energy supply.

Currently, available retorting technologies for the production of oil and gas from oil shale globally are classified into aboveground retorting and underground retorting. The aboveground retorting technology involves building a large-scale furnace on the ground to create a high-temperature anaerobic environment. Then, oil shale mined from underground is crushed to a certain size, sent to the furnace and retorted to obtain shale oil and hydrocarbon gases [7–11]. This requires large land areas and incurs high mining costs, no matter the mining method. It also produces solid waste residues, wastewater and noxious gases during the refining process [12–15]. In 2008, China's output of shale oil produced by the aboveground retorting technology was only 0.375 million tons [1]. With this amount, shale oil was far from being a substitute for crude oil. Nowadays, global energy companies are actively developing new economic and environmentally friendly underground retorting technologies to extract oil and gas from the oil shale seam by using various in-situ heating methods. This approach has become recognized as being effective for a large-scale commercial production of oil from oil shale. Today, well-known in-situ heating technologies include Shell's in-situ conversion process (ICP), Electrofrac™, CRUSH, LLNL, GFC, and in-situ steam injection (MTI) [16–24]. Of these, only the ICP technology has been industrially tested, in the Piceance Basin, Colorado [21, 22]. The basic principle of ICP is that oil shale deposits are heated by the electric heating apparatus installed in boreholes so that organic matter can be pyrolyzed to give oil and gas whose products are then transported out of the production well. However, some technical disadvantages of this technology limit its global implementation. First, conduction is the main mode of heat transfer in oil shale, but its efficiency is very low [25, 26]. Second, the active migration ability of oil and gas is weak [21]. Third, the electric heating components in the constant heating process are extremely prone to malfunction, resulting in low service life and high maintenance costs. Fourth, electricity is an advanced energy source, however, higher power consumption increases development cost. Therefore, it is critical and urgent to develop an economically feasible in-situ retorting technology for oil and gas extraction from oil shale.

2. Oil shale in-situ steam injection technology

Scientists at Taiyuan University of Technology have been engaged for many years in the development of the technology and theory of oil shale underground retorting, as well as in the related experimental research [27–32]. In 2010, the researchers were granted a Chinese patent titled "The method for extracting oil & gas from oil shale by convection heating" [24]. The technical scheme of the technology may be outlined as follows: 1) arranging of wells on the ground and drilling down to the oil shale layer, connecting of injection and production wells by hydraulic fracturing; 2) injecting of superheated steam (T > 500 °C) generated inside a boiler into the oil shale layer down the injection well via a surface pipe network, heating and pyrolyzing of organic matter to produce oil and gas; (3) flowing of the hot mixed fluid containing oil, gas and steam along the cracks to the production well and discharging it to a low-temperature power generation system to generate electricity, then separating the fuid to obtain oil and gas, and recycling of water after purification. The main technical process of the MTI technology is illustrated in Figure 1.

A detailed analysis of the principle of the MTI technology suggests that its on-site implementation has many technical advantages, as shown below:

(1) Large cracks formed by hydraulic fracturing guarantee smooth exploitation from the beginning of heat injection. Once the pyrolytic process reaches the normal operation stage, large pores and fracture channels are produced through thermal cracking and continuous pyrolysis of organic matter, ensuring a sustainable implementation of the in-situ retorting process [32, 33].
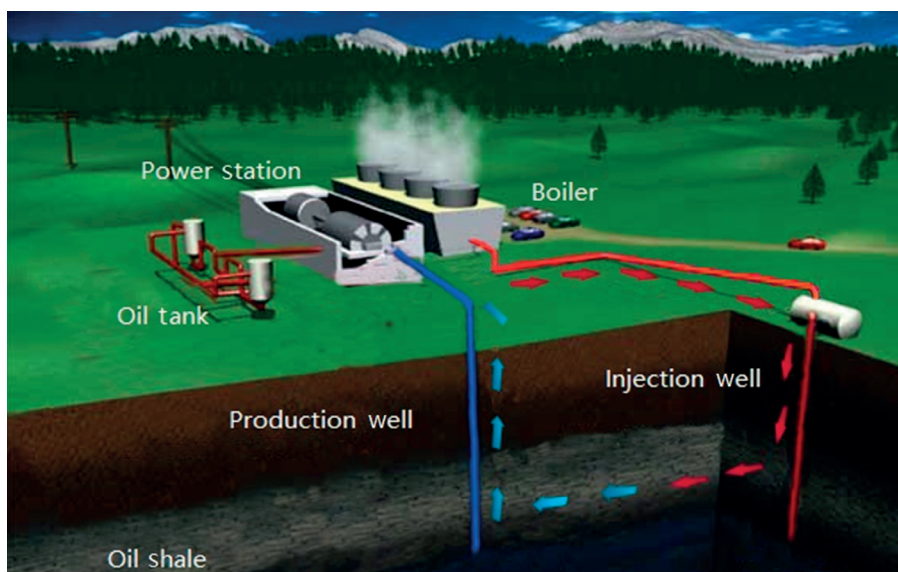

Fig. 1. Schematic of MTI technology.

(2) Convection heat transfer of superheated steam enhances the efficiency of heating the oil shale layer, which significantly shortens the time to achieve a complete pyrolysis of organic matter [33].

(3) Under the influence of steam the migration capacity of oil and gas is improved and their products are carried out of the production well rapidly. This results in a relatively high recovery rate of oil and gas [33].

(4) According to the temperature of the oil shale layer, all the wells in the network are alternately used as the injection well for injecting superheated steam to ensure an efficient heating of the oil shale layer, while the target pyrolysis area of the latter can be flexibly controlled [33].

(5) On completion of steam injection, a large amount of skeletal semi-coke residue remaining underground does not cause any land subsidence hazard.

(6) Using water steam as a heat carrier fluid to pyrolyze oil shale allows easy separation of water as well as oil and gas products by applying the cooling separation technology. In addition, water is recycled after simple purification, which has economic benefits.

To further verify the feasibility of MTI for oil shale underground retorting, we conducted a heating and pyrolysis experiment on oil shale using superheated steam (up to 570 °C), and further numerically simulated its in-situ steam injection process.

3. Heating and pyrolysis experiment on oil shale using superheated steam

3.1. Experimental samples

The oil shale samples used for the experiment were collected from Fukang City, Xinjiang Province, China. The samples were encased in paraffin in the field to prevent weathering and denudation, then delivered to the laboratory.

3.2. Experimental arrangement

In this work, the steam pyrolysis test was carried out using a high-temperature steam pyrolysis test bench (Fig. 2) independently developed by Wang et al. at Taiyuan University of Technology [34]. As displayed in Figure 2, the experimental system for oil shale heating and pyrolysis using superheated steam consists of a steam generator, superheating pipe, retort, condensing tube, and temperature/pressure monitoring sensor. The control sensitivity of temperature and pressure are 0.1 °C and 0.01 MPa, respectively. Kök et al. [35] reported a steam injection pyrolysis test on Turkish oil shale and found that steam injection was not feasible for this purpose. However, the steam temperature in those experiments was only 180 °C, well below the temperature necessary to pyrolyze organic matter in oil shale. By contrast, the temperature of superheated steam in the experimental system used in the current work may amount to 570 °C, which is enough to pyrolyze organic matter in oil shale completely.

(a)

(b)
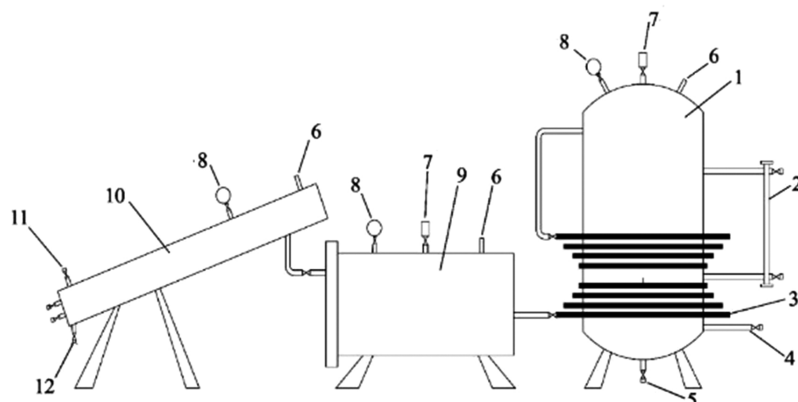
1 – steam generator, 2 – water level gauge, 3 – superheating pipe, 4 – water intake,
5 – drain outlet, 6 – temperature sensor, 7 – safety valve, 8 – pressure gauge, 9 – retort,
10 – condensing tube, 11 – gas exhaust valve, 12 – shale oil drain valve.

Fig. 2. Photograph (a) and schematic (b) of the high-temperature steam pyrolysis test bench.

3.3. Experimental method

Initially, 10 kg of oil shale samples was transferred to the retort and the steam generator was charged with water to a predetermined level using an electric pump. Superheated steam was produced by burning natural gas to heat the steam generator and superheated tube, the temperature/pressure monitoring and condensation circulation systems were simultaneously working. Superheated steam was then continuously injected into the retort to pyrolyze the samples at temperatures up to 570 °C for 70 min. The steam carrying oil and gas generated at different temperatures was condensed in the condensing tube and collected separately for laboratory analysis.

After pyrolysis, the composition of generated gas was determined by the Agilent 7890A gas chromatography (GC) system following the GB/T 13610-2014 standard [36]. The volatile liquid hydrocarbons (C_5–C_{35}) of shale oil were determined by the HP6890 GC System equipped with an HP-5MS column and a Flame Ionization Detector (FID). The detailed analytical procedures of hydrocarbons in shale oil were carried out following the SY/T 5779-2008 standard [37]. The oven temperature was run at 40 °C with an isothermal period of 10 min. Subsequently the temperature program was run from 40 °C to 310 °C at a rate of 5 °C and then held at 310 °C for 30 min. In both GC experiments, helium was used as a carrier gas.

3.4. Experimental results

The retort was opened after cooling down to room temperature and the semi-coke in the retort was removed and weighed. The final weight of semi-coke was 8.35 kg; thus, the total weight loss was 1.65 kg (16.5%).

Table 1. Fischer assay of Fukang oil shale and semi-coke

Location	Sample	Water, %	Ash, %	Oil content, %	Gas + loss, %
Fukang City	Original oil shale	1.12	89.6	7.02	2.26
	Semi-coke	0.40	99.3	0.14	0.16

Oil content is an important technical index for assessing the economic value of oil shale. The oil content of semi-coke is used to evaluate the oil recovery rate in the pyrolysis process. Thus, the original Fukang oil shale sample and its pyrolysis residue semi-coke were both subjected to Fischer Assay analysis for oil content determination. Table 1 reveals that the oil content of the original oil shale sample was 7.02% and that of semi-coke after superheated steam pyrolysis only 0.14%, implying that the residual organic matter content of the latter was extremely low. However, when superheated steam was used to heat and pyrolyze the Fukang oil shale, the oil recovery rate was higher than 95%. Figure 3 shows the images of Fukang oil shale samples before and after pyrolysis by superheated steam. A large number of internal fractures parallel to the bedding direction appear in the samples after heating and pyrolysis. The newly formed fractures provide unobstructed seepage channels for steam injection and oil and gas production.
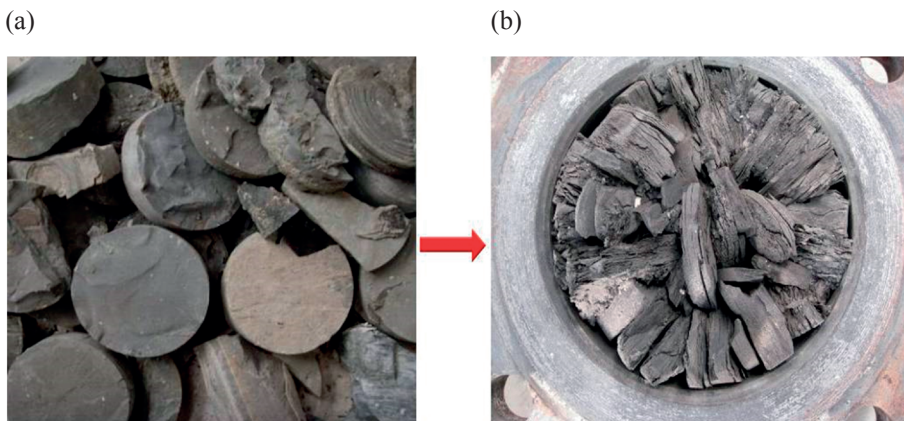
(a)　　　　　　　　　　　　　　　(b)

Fig. 3. Images of Fukang oil shale samples before (a) and after (b) pyrolysis by superheated steam.

The carbon numbers (C_n) of organic compounds contained in the shale oil generated by the experiment are listed in Table 2. It can be seen that C_n is between C_5 and C_{35}. Based on chemical structure, the compounds were divided into two types: saturated hydrocarbons (*n*-alkanes) and unsaturated hydrocarbons (*n*-olefins and iso-olefins). The proportion of *n*-alkanes in shale oil was the highest, accounting for 68.523% of total composition, while *n*-olefins and iso-olefins formed 24.7973% and 6.6796%, respectively.

The data given in Table 2 was used to construct the curves of shale oil compounds distribution (Fig. 4). The figure shows the compounds to have a normal distribution, with the main peak at C_{11}. Carbon numbers C_5, C_{10}, C_{11}, C_{13}, C_{14}, C_{18}, C_{19}, C_{25}, C_{26} and C_{35} were taken as demarcation points to divide shale oil into oil components: gasoline (C_5–C_{10}), kerosene (C_{11}–C_{13}), diesel (C_{14}–C_{18}), paraffin oil (C_{19}–C_{25}) and lubricating oil (C_{26}–C_{35}). Gasoline, kerosene and diesel are light oils, paraffin oil and lubricating oil are heavy oils. The relatively high proportions of gasoline (19.96%), kerosene (24.32%) and diesel (31.10%) imply that shale oil is mainly composed of light oils (75.38% in total). This indicates that the quality of shale oil is significantly improved by superheated steam pyrolysis. The main reason is that the aquathermolysis interaction between superheated steam and asphaltene breaks the long-chain hydrocarbons in organic matter and synthesizes its short-chain hydrocarbons by combining the latter with a large number of free hydrogen ions in superheated steam, which greatly increases the proportion of light oil components in shale oil [38].

Table 2. Carbon number distribution in Fukang shale oil compounds

| C number	n-alkanes, %	n-olefins, %	iso-olefins, %	Total hydrocarbons, %
C_5	0.0030	0.0000	0.0000	0.0300
C_6	0.0598	0.0278	0.0162	0.1038
C_7	0.7033	0.2909	0.1187	1.1128
C_8	2.4121	0.9990	0.3528	3.7638
C_9	4.0614	1.7868	0.8177	6.6659
C_{10}	5.1908	2.2363	0.8855	8.3127
C_{11}	5.4048	2.4166	0.8076	8.6289
C_{12}	5.2441	2.1963	0.4335	7.8739
C_{13}	5.2847	2.0964	0.4342	7.8152
C_{14}	4.9371	1.9439	0.3474	7.2284
C_{15}	4.6693	1.8017	0.3367	6.8077
C_{16}	4.3251	1.3997	0.4220	6.1468
C_{17}	4.2388	1.3545	0.2581	5.8514
C_{18}	3.6699	1.0955	0.301	5.0664
C_{19}	3.5986	1.0556	0.2445	4.8987
C_{20}	2.9223	0.8884	0.2297	4.0404
C_{21}	2.5349	0.8251	0.2207	3.5807
C_{22}	1.9498	0.6579	0.1968	2.8044
C_{23}	1.6242	0.4455	0.1314	2.2011
C_{24}	1.2061	0.3251	0.1253	1.6565
C_{25}	1.0059	0.3633	0.0000	1.3692
C_{26}	0.784	0.2681	0.0000	1.0521
C_{27}	0.6305	0.1790	0.0000	0.8095
C_{28}	0.5952	0.1440	0.0000	0.7392
C_{29}	0.4927	0.0000	0.0000	0.4927
C_{30}	0.3152	0.0000	0.0000	0.3152
C_{31}	0.2011	0.0000	0.0000	0.2011
C_{32}	0.165	0.0000	0.0000	0.1650
C_{33}	0.1355	0.0000	0.0000	0.1355
C_{34}	0.0863	0.0000	0.0000	0.0863
C_{35}	0.0718	0.0000	0.0000	0.0718
Total	68.5230	24.7973	6.6796	100.00
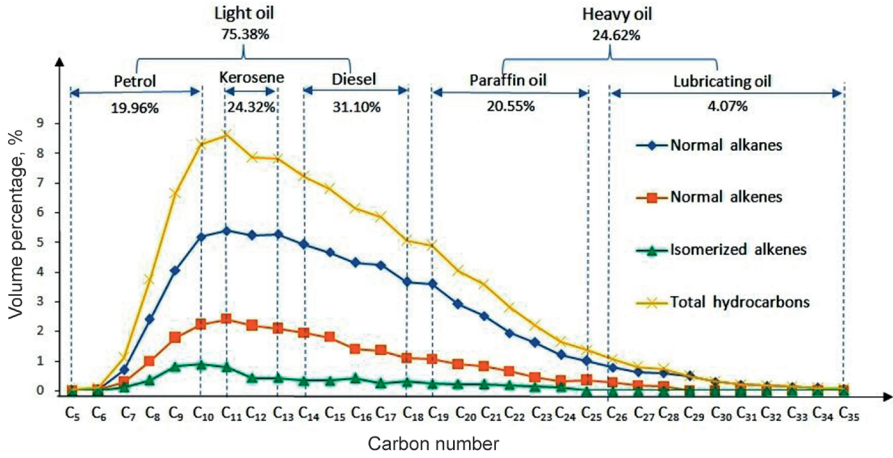
Fig. 4. Composition of shale oil from high-temperature superheated steam pyrolysis of Fukang oil shale.

Figure 5 shows the change in gas volume with steam temperature during the experiment. The gas flowmeter did not detect any pyrolysis gas generation until the steam temperature reached 280 °C, after which its formation by small amounts only was recorded. The gas production increased then rapidly at temperatures from 350 °C to 460 °C. At 570 °C, the total gas volume was 0.41 m³ (i.e. gas production per unit mass was 0.041 m³/kg), and the gas production rate was 9.76×10^{-6} m³/(kg s) during the experiment.
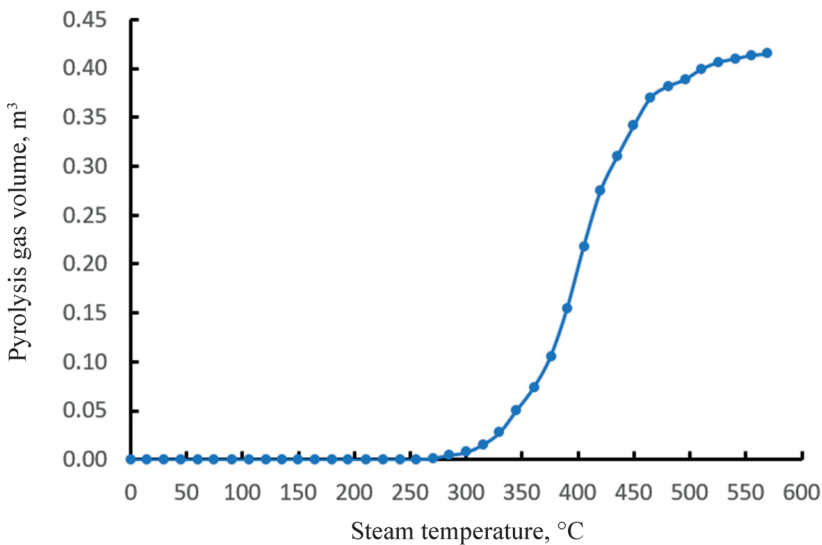

Fig. 5. Cumulative gas production vs temperature increase.

The composition and volumetric contents of the gas generated at different temperatures were determined by gas chromatography (Fig. 6). The pyrolysis gas was found to consist mainly of hydrocarbon (CH_4, C_2H_6, C_2H_4, C_3H_8) and non-hydrocarbon (CO_2, CO, H_2) gases. As shown in Figure 6, the volume content of hydrocarbon gases trended similarly with increasing temperature, initially increasing and then decreasing, with a peak value at about 375 °C. Among them, CH_4 had the highest volume content, reaching about 20% at 375 °C. The volume content of non-hydrocarbon gases remained relatively high; the content variation trends of individual compounds were different with increasing temperature. The volume content of CO_2 initially decreased rapidly, reaching its lowest value at 360 °C, then increased with rising temperature. The volume content of CO fluctuated around 5% below 450 °C, then increased with temperature to 8.30% at 570 °C. H_2 was a major constituent of pyrolytic gases, and its volume content showed a rising trend with increasing temperature, with a peak of 52.26% at 570 °C.

The variation in the volume content of individual pyrolysis gas components is explained by the high reducibility of most free hydrogen ions existing in superheated steam at temperatures above 450 °C, which indicates that the steam reacts vigorously with the fixed-carbon in semi-coke. Therefore, the volume content of H_2 and CO increased significantly, improving both the yield and calorific value of pyrolytic gases.
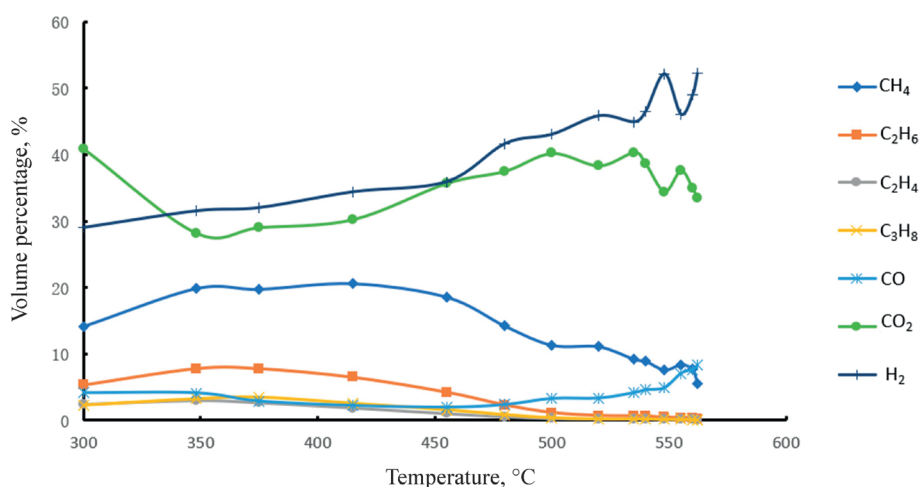

Fig. 6. Variations in the volume content of pyrolysis gas components.

4. Numerical simulation of oil shale in-situ steam injection

4.1. Physical model

For numerical simulation the physical properties of the rock and other parameters given in Table 3 were used. Three rock formations were considered in the model, from bottom to top: floor (0–15 m), oil shale seam (15–40 m) and roof (40–55 m). A hydraulic fracture 0.04 m wide was placed at 27.48–27.52 m in the center of the oil shale formation. The injection and production wells were 40 m deep and 50 m apart in the model (Fig. 7), and were alternately used for steam injection on day 201 (Fig. 8). The boundary and initial conditions are summarized as follows (Fig. 8):

   • The initial temperature of rock formation: $T(x, y, t = 0) = 30\ °C$
   • The initial pore pressure of rock formation: $P(x, y, t = 0) = 0.1\ MPa$
   • The steam temperature at the injection section:
$T(x = 0\ m, y = 15–40\ m, t = 0–200\ d) = 600\ °C$
$T(x = 50\ m, y = 15–40\ m, t = 201–300\ d) = 600\ °C$
   • The steam pressure at the injection section:
$P(x = 0\ m, y = 15–40\ m, t = 0–200\ d) = 3.0\ MPa$
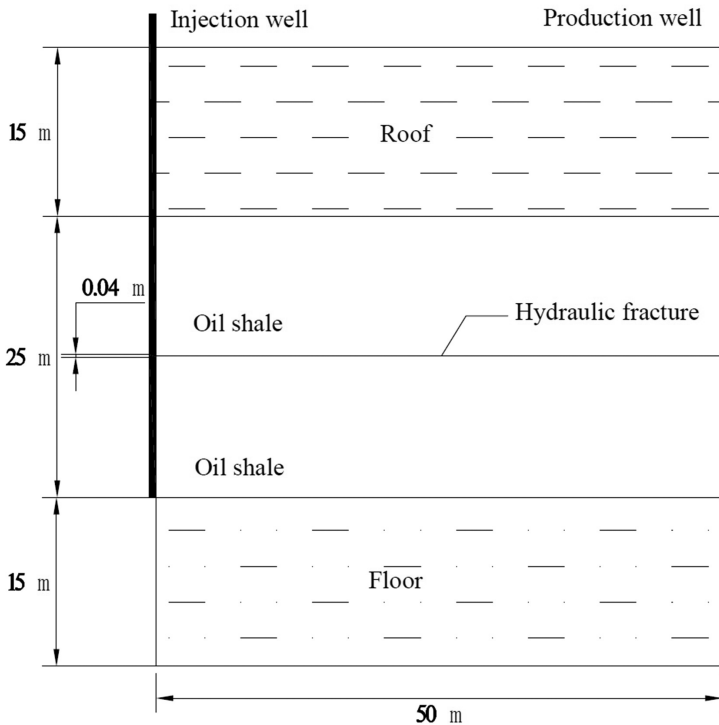$P(x = 50\ m, y = 15–40\ m, t = 201–300\ d) = 3.0\ MPa.$
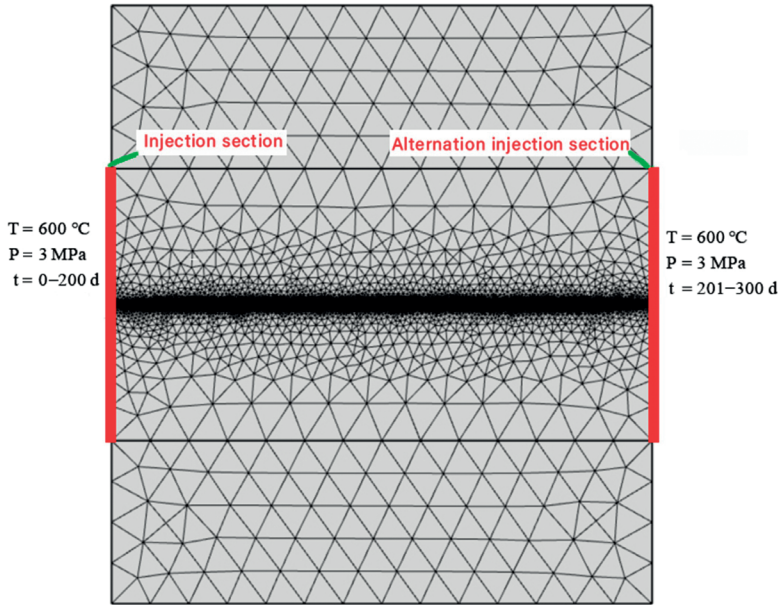

Fig. 7. Physical model diagram.

Fig. 8. Mesh and steam injection conditions.

Table 3. Numerical simulation conditions [39–42]

Physical characteristic/parameter	Oil shale	Roof and floor	Hydraulic fracture
Porosity	0.09	0.04	0.43
Permeability, m^2	4.8×10^{-15}	1.0×10^{-15}	3.2×10^{-13}
Density, kg/m^3	1.9×10^3	2.2×10^3	
Thermal conductivity, $W/(m \cdot K)$	0.75	0.43	
Specific heat, $J/(kg \cdot K)$	1.31×10^3	0.85×10^3	
Chemical reaction heat, J/kg	176×10^3		
Gas production rate, $m^3/(kg \cdot s)$	9.76×10^{-6}		

4.2. Numerical model

Oil shale is a typical porous medium at high temperature. Based on the theory of heat transfer and seepage in porous media, the constitutive mathematical models of seepage-thermal coupling for in-situ pyrolysis of oil shale by injecting superheated steam are as follows [39–41]:

The seepage equation is:

$$\left(k_i p_{,i}^2\right)_{,i} = n\frac{\partial p}{\partial t} + w, \tag{1}$$

the heat transfer equation for porous media is:

$$(1-n)\rho_r C_r \frac{\partial T}{\partial t} = (1-n)\lambda_r T_{,ii} + Q_s, \tag{2}$$

the heat transfer equation for steam is:

$$\begin{cases} n\rho_g C_g \dfrac{\partial T}{\partial t} + \rho_g C_g k_i p_{,i} T_{,i} = n\lambda_g T_{,ii} + Q_g \\ \rho_g = \dfrac{Mp}{RTZ} \end{cases}, \tag{3}$$

where p is the steam pressure, Pa; k is the permeability, m·s^{-1}; n is the porosity, %; w is the gas volume pyrolyzed from kerogen, m^3·kg^{-1}·s^{-1}; p_r is the density of rock, kg·m^{-3}; C_r is the specific heat of rock at constant pressure, J·kg^{-1}·k^{-1}; T is the temperature, °C; λ_r is the thermal conductivity of rock, W·m^{-1}·k^{-1}; Q_s is the chemical reaction heat, J·kg^{-1}; p_g is the steam density, kg·m^{-3}; C_g is the specific heat of steam at constant pressure, J·kg^{-1}·k^{-1}; λ_g is the thermal conductivity of steam, W·m^{-1}·k^{-1}; Q_g is the thermal source or heat sink item of the gas, J·kg^{-1}; M is the molecular weight of steam; R is the molar gas constant, 8.314 J·mol^{-1}·k^{-1}; and Z is the gas compressibility factor.

4.3. Seepage field analysis

The oil shale in-situ steam injection process was simulated for 300 days (Fig. 9). When steam is injected into the oil shale reservoir, firstly, it flows rapidly along the pre-existing fracture at the center of the oil shale reservoir, then, mixed with oil and gas, is discharged from the production well. Over time, pressure gradually spreads to the regions on both sides of the fracture. The pressure gradient is relatively high within 18 m of the injection well (Fig. 9c) where steam flows rapidly, resulting in highly significant heat transfer by convection. Because the roof and floor rocks do not exhibit obvious thermal cracking [33], their permeability is lower than that of the oil shale seam, and the pressure in the roof and floor rises slowly, showing obvious hysteresis characteristics, which have an effective sealing effect on the steam. To increase the efficiency of heat transfer in the oil shale reservoir near the production
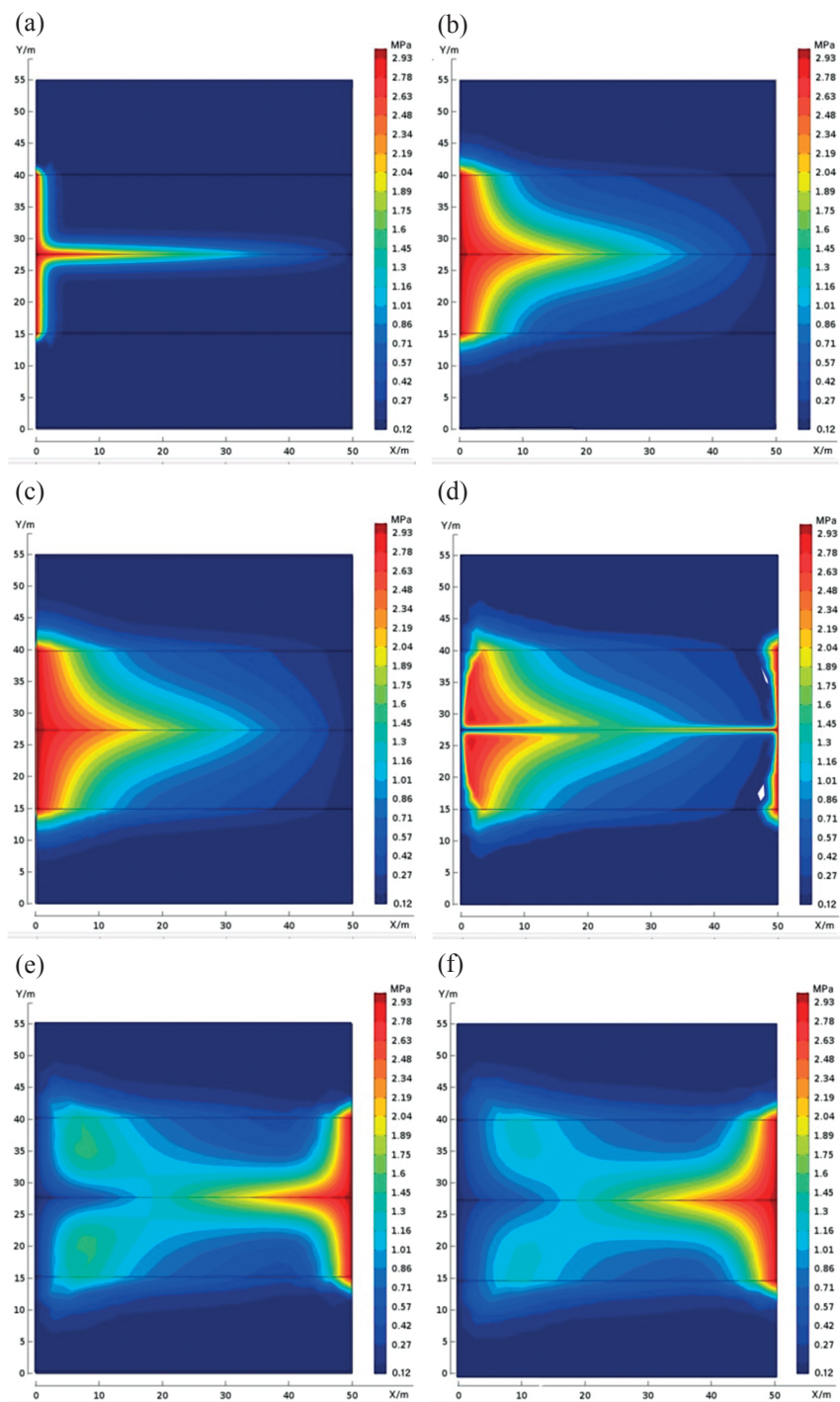
Fig. 9. Reservoir pressure profiles at different pyrolysis times: (a) t = 10 days; (b) t = 120 days; (c) t = 200 days; (d) t = 201 days; (e) = 260 days; (f) = 300 days.

well, the latter was used as an injection well to inject steam from day 201. This resulted in a rapid increase of pressure gradient in the oil shale reservoir within a horizontal range of 30–50 m (Fig. 9e), which significantly improved the pyrolysis efficiency in the target area. Finally, the steam injection was terminated on day 300.

4.4. Temperature distribution analysis

In the process of steam convection heating, the temperature of the oil shale reservoir is directly controlled by the steam seepage field, so the morphology of the temperature distribution in the reservoir is similar to that of the seepage field (Fig. 10). When steam is injected into the oil shale reservoir, the temperature of the oil shale near the fracture surface rapidly exceeds 500 °C (Fig. 10a), and oil and gas products carried by steam are rapidly produced in the production well. It can be concluded that oil and gas products are quickly obtained using the MTI technology with no preheating required. Over time, the temperature of oil shale on both sides of the fracture surface rises rapidly. After 200 days of continuous heat injection, oil shale within 20 m near the injection well has been basically pyrolyzed.

On day 201, the production well was used as an injection well (Fig. 10d). Then, after a further 100 days of continuous steam injection, the remaining region of the oil shale reservoir was also substantially pyrolyzed. The high-temperature zone in the rock formations was mainly concentrated in the oil shale reservoir and its overall temperature exceeded 480 °C. This indicates that the pyrolysis of the oil shale reservoir was complete after 300 consecutive days of steam injection in this model, which confirms that the energy carried by superheated steam was mainly utilized in the pyrolysis of organic matter contained in oil shale. Besides, the temperature of the upper boundary (roof) and the lower boundary (floor) remained at about 30 °C, indicating that they may provide effective thermal insulation and steam imperviousness.
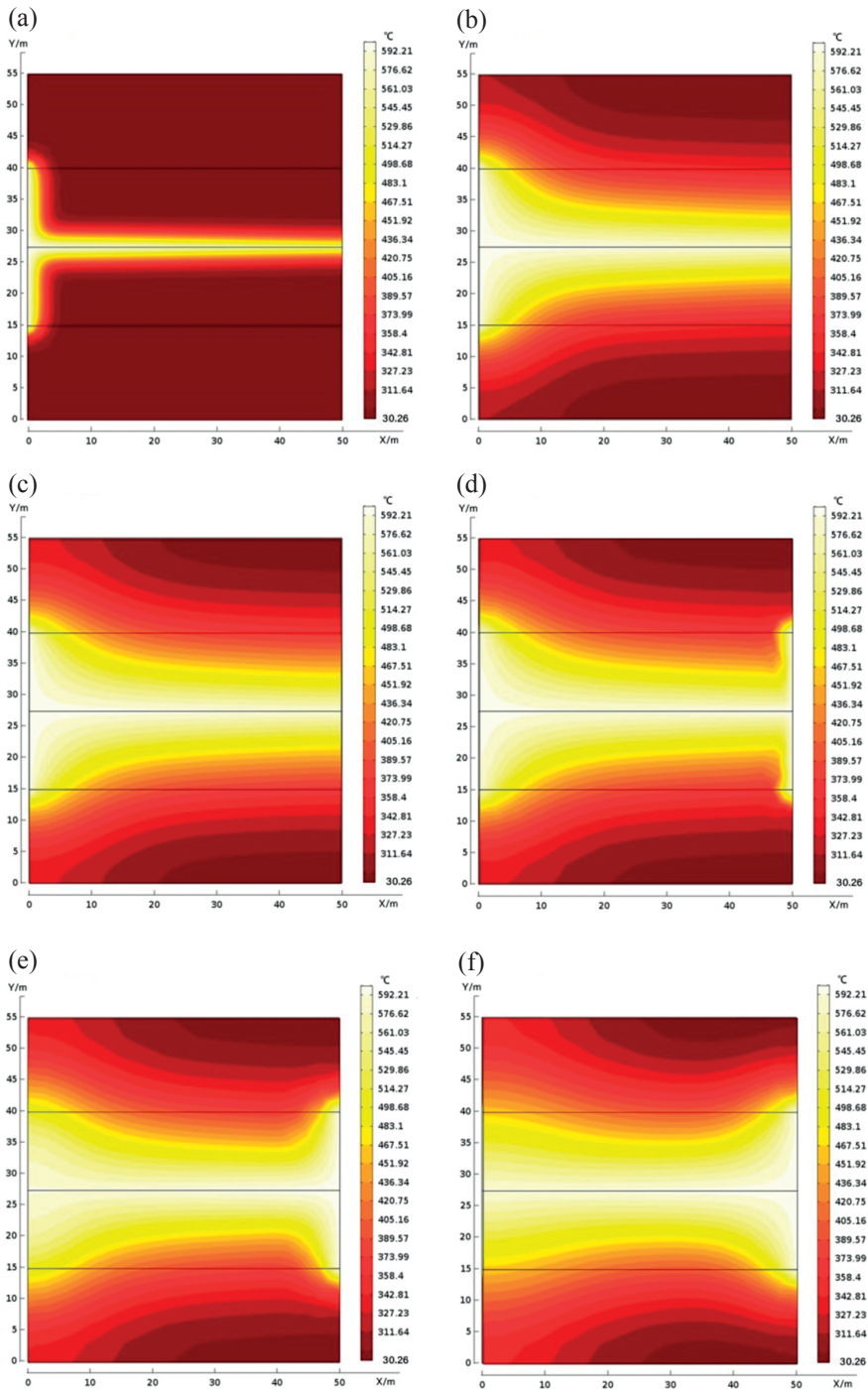
Fig. 10. Reservoir temperature profiles at different pyrolysis times: (a) t = 10 days; (b) t = 120 days; (c) t = 200 days; (d) t = 201 days; (e) t = 260 days; (f) t = 300 days.

5. Conclusions

In summary, the aboveground oil shale retorting technology has numerous limitations, such as high cost, environmental pollution hazard and low production capacity. In contrast, the in-situ steam injection technology represents a novel process for the underground retorting of oil shale to extract oil and gas, whose successful implementation may alleviate the energy crisis in China and reduce the country's dependence on imported petroleum. However, the entire implementation process of the new technology is a complex and systematic procedure, which needs considering many factors such as oil shale oil content, ore thickness, hydrogeological conditions, and cost, as well as conducting a related in-depth study. This paper introduced the basic principles and advantages of the novel technology and proved its feasibility for oil shale underground retorting through a superheated steam pyrolysis experiment and numerical simulation of in-situ steam injection. The main conclusions are as follows:

1. Convection heat transfer of steam enhances the efficiency of heating the oil shale layer, which shortens the time to achieve a complete pyrolysis of organic matter. Under the influence of steam the migration capacity of oil and gas is improved and as a result, their products are carried rapidly out of the production well. Moreover, oil and gas products can be easily obtained through a simple condensation separation process.

2. By using superheated steam (up to 570 °C) to pyrolyze oil shale, the oil recovery rate may exceed 95% with the gas production per unit mass of 0.041 m^3/kg, and, at the same time, the quality of oil and gas products can be greatly improved. The proportion of light oils in shale oil accounts for 75.38%, and the yield of H_2 and CO in pyrolysis gases is increased.

3. The results of numerical simulation indicate that the novel in-situ steam injection technology is a rapid and efficient method for oil shale underground retorting to extract oil and gas by using the injection and production wells alternately for injecting steam. The development period of the technology is only about 300 days for the oil shale reservoir with a well spacing of 50 m, and the roof and floor of the oil shale layer provide good thermal insulation and act as the steam barrier.

REFERENCES

1. Dyni, J. R. Oil Shale. In: *2010 Survey of Energy Resources Executive Summary*. World Energy Council, 2010.
2. Kök, M. V., Pamir, M. R. Non-isothermal pyrolysis and kinetics of oil shales. *J. Therm. Anal. Calorim.*, 1999, **56**(2), 953–958.
3. Kök, M. V. Heating rate effect on the DSC kinetics of oil shales. *J. Therm. Anal. Calorim.*, 2007, **90**(3), 817–821.
4. Li, S. Y., Yue, C. T. Study of pyrolysis kinetics of oil shale. *Fuel*, 2003, **82**(3), 337–342.
5. Qian, J. L., Yin, L., Li, S. Y. *Oil Shale – Petroleum Alternative*. China Petrochemical Press, Beijing, 2010.
6. Liu, Z. J., Meng, Q. T., Dong, Q. S., Zhu, J. W., Guo, W., Ye, S. Q., Liu, R., Jia, J. L. Characteristics and resource potential of oil shale in China. *Oil Shale*, 2017, **34**(1),15–41.
7. Wang, S., Jiang, X. M., Han, X. X., Tong, J. H. Investigation of Chinese oil shale resources comprehensive utilization performance. *Energy*, 2012, **42**(1), 224–232.
8. Golubev, N. Solid oil shale heat carrier technology for oil shale retorting. *Oil Shale*, 2003, **20**(3S), 324–332.
9. Li, X., Zhou, H., Wang, Y., Qian, Y., Yang, S. Thermoeconomic analysis of oil shale retorting processes with gas or solid heat carrier. *Energy*, 2015, **87**, 605–614.
10. Karu, V., Västrik, A., Anepaio, A., Väizene, V., Adamson, A., Valgma, I. Future of oil shale mining technology in Estonia. *Oil Shale*, 2008, **25**(2S), 125–134.
11. Pan, Y., Zhang, X. M., Liu, S. H., Yang, S. C., Ren, N. A review on technologies for oil shale surface retort. *J. Chem. Soc. Pakistan*, 2012, **34**(6), 1331–1338.
12. Selberg, A., Viik, M., Pall, P., Tenno, T. Environmental impact of closing of oil shale mines on river water quality in North-Eastern Estonia. *Oil Shale*, 2009, **26**(2), 169–183.
13. Reinik, J., Irha, N., Steinnes, E., Piirisalu, E., Aruoja, V., Schultz, E., Leppänen, M. Characterization of water extracts of oil shale retorting residues from gaseous and solid heat carrier processes. *Fuel Process. Technol.*, 2015, **131**, 443–451.
14. Nei, L., Kruusma, J., Ivask, M., Kuu, A. Novel approaches to bioindication of heavy metals in soils contaminated by oil shale wastes. *Oil Shale*, 2009, **26**(3), 424–431.
15. Kuusik, R., Martins, A., Pihu, T., Pesur, A., Kaljuvee, T., Prikk, A., Trikkel, A., Arro, H. Fluidized-bed combustion of oil shale retorting solid waste. *Oil Shale*, 2004, **21**(3), 237–248.
16. Crawford, P., Biglarbigi, K., Dammer, A., Knaus, E. Advances in world oil-shale production technologies. In: *SPE Annual Technical Conference and Exhibition (ATCE 2008)*, September 21–24, 2008 Denver, Colorado, USA, vol. 6, SPE 116570, 4101–4111.
17. Brandt, A. R. Converting oil shale to liquid fuels: energy inputs and greenhouse gas emissions of the Shell in situ conversion process. *Environ. Sci. Technol.*, 2008, **42**(19), 7489–7495.

18. Crawford, P., Killen, J. New challenges and directions in oil shale development technologies. In: *Oil Shale: Solutions to the Liquid Fuel Dilemma* (Ogunsola, O. I., Hartstein, A. M., Ogunsola, O., eds.). ACS Sym. Ser., **1032**, 21–60, Oxford University Press, 2010.

19. Symington, W. A., Olgaard, D. L., Otten, G. A., Phillips, T. C., Thomas, M. M., Yeakel, J. D. ExxonMobil's electrofrac process for in situ oil shale conversion. In: *Oil Shale: Solutions to the Liquid Fuel Dilemma* (Ogunsola, O. I., Hartstein, A. M., Ogunsola, O., eds.). ACS Sym. Ser., **1032**, 185–216, Oxford University Press, 2010.

20. Vinegar, H. Shell's in-situ conversion process. In: *Proceedings of the 26th Oil Shale Symposium*, October 16–18, 2006, Colorado School of Mines, Golden, Colorado, 2006.

21. Fowler, T. D., Vinegar, H. J. Oil shale ICP – Colorado field pilots. In: *SPE Western Regional Meeting*, San Jose, CA, March 24–26, 2009. Society of Petroleum Engineers, 2009.

22. Ryan, R. C., Fowler, T**.** D., Beer, G. L., Nair, V. N. Shell's in situ conversion process – from laboratory to field pilots. In: *Oil Shale: Solutions to the Liquid Fuel Dilemma* (Ogunsola, O. I., Hartstein, A. M., Ogunsola, O., eds.). ACS Sym. Ser., **1032**, 161–183, Oxford University Press, 2010.

23. Tanaka, P. L., Yeakel, J. D., Symington, W. A., Spiecker, P. M., Del Pico, M., Thomas, M. M., Sullivan, K. B., Stone, M. T. Plan to test ExxonMobil's *in situ* oil shale technology on a proposed RD&D lease. In: *31st Annual Oil Shale Symposium*, Colorado School of Mines, October 17–19, 2011.

24. Zhao, Y., Feng, Z., Yang, D., Liu, S., Sun, K., Zhao, J., Guan, K., Duan, K. *The Method for Extracting Oil & Gas from Oil Shale by Convection Heating*. China Patent, CN200510012473, 4, 2010 (in Chinese).

25. Kang, Z. Q., Zhao, Y. S., Yang, D. Physical principle and numerical analysis of oil shale development using in-situ conversion process technology. *Acta Petrolei Sinica*, 2008, **29**(4), 592–595 (in Chinese).

26. Han, H., Zhong, N. N., Huang, C. X., Liu, Y., Luo, Q. Y., Dai, N., Huang, X. Y. Numerical simulation of in situ conversion of continental oil shale in Northeast China. *Oil Shale*, 2016, **33**(1), 45–57.

27. Geng, Y., Liang, W., Liu, J, Cao, M., Kang, Z. Evolution of pore and fracture structure of oil shale under high temperature and high pressure. *Energ. Fuel.*, 2017, **31**(10), 10404–10413.

28. Wang, G., Yang, D., Zhao, Y., Kang, Z., Zhao, J., Huang, X. Experimental investigation on anisotropic permeability and its relationship with anisotropic thermal cracking of oil shale under high temperature and triaxial stress. *Appl. Therm. Eng.*, 2019, **146**, 718–725.

29. Wang, L., Yang, D., Zhao, J., Zhao, Y., Kang, Z. Changes in oil shale characteristics during simulated in-situ pyrolysis in superheated steam. *Oil Shale*, 2018, **35**(3), 230–241.

30. Wang, L., Yang, D., Li, X., Zhao, J., Wang, G., Zhao, Y. Macro and meso characteristics of in-situ oil shale pyrolysis using superheated steam. *Energies*, 2018, **11**(9), 2297.

31. Kang, Z., Zhao, J., Yang, D., Zhao, Y., Hu, Y. Study of the evolution of micron-scale pore structure in oil shale at different temperatures. *Oil Shale*, 2017, **34**(1), 42–55.

32. Wang, L., Zhao, Y., Yang, D., Kang, Z., Zhao, J. Effect of pyrolysis on oil shale using superheated steam: A case study on the Fushun oil shale, China. *Fuel*, 2019, **253**, 1490–1498.

33. Kang, Z., Zhao, Y., Yang, D., Tian, L., Li, X. A pilot investigation of pyrolysis from oil and gas extraction from oil shale by *in-situ* superheated steam injection. *J. Petrol. Sci. Eng.*, 2020, **186**, 106785.

34. Wang, Y., Zhao, Y., Feng, Z. Study of evolution characteristics of pore structure during flame coal pyrolysis. *Chinese Journal of Rock Mechanics and Engineering*, 2010, **29**(9), 1859–1866 (in Chinese).

35. Kök, M. V., Guner, G., Bagci, S. Laboratory steam injection applications for oil shale fields of Turkey. *Oil Shale*, 2008, **25**(1), 37–46.

36. GB/T 13610-2014. *Analysis of Natural Gas Composition – Gas Chromatography*. Research Institute of Standards & Norms, Beijing, China, 2014 (in Chinese).

37. SY/T 5779-2008. *Analytical Method of Hydrocarbons in Petroleum and Sediment by Gas Chromatography*. National Development and Reform Commission, Beijing, China, 2008 (in Chinese).

38. El Harfi, K., Mokhlisse, A., Chanâa, M. B. Effect of water vapor on the pyrolysis of the Moroccan (Tarfaya) oil shale. *J. Anal. Appl. Pyrol.*, 1999, **48**(2), 65–76.

39. Hao, Y., Yunxing, D. A feasibility study on in-situ heating of oil shale with injection fluid in China. *J. Petrol. Sci. Eng.*, 2014, **122**, 304–317.

40. Lee, K, J., Moridis, G. J., Ehlig-Economides, C. A. Oil shale in-situ upgrading by steam flowing in vertical hydraulic fractures. *SPE Unconventional Resources Conference*, 1–3 April 2014, The Woodlands, Texas, USA. Society of Petroleum Engineers, 2014.

41. Kang, Z. Q. *The Pyrolysis Characteristics and In-Situ Hot Drive Simulation Research That Exploit Oil-Gas of Oil Shale*. PhD Thesis, Taiyuan University of Technology (in Chinese).

42. Qian, J. L., Yin, L., Wang, J. Q. *Oil Shale-Complementary Energy of Petroleum*. China Petrochemical Press, Beijing, 2008 (in Chinese).